eNergetics 2025
DOI: https://doi.org/10.5281/zenodo.18624313

Original Scientific Article

Interface Defect Layer Engineering for Realistic Modeling of 2D/3D Mixed Dimensional Perovskite Solar Cells

Walagedara Gamage Ayomi Pabasara[1], Galhenage Asha Sewvandi[2]

[1,2]Department of Materials Science and Engineering, University of Moratuwa, Katubedda, Sri Lanka
[1]Department of Engineering Technology, University of Ruhuna, Kamburupitiya, Sri Lanka

[1]ayomi@fot.ruh.ac.lk, [2]galhenagea@uom.lk

Abstract—**This study focuses on a comprehensive investigation into the influence of interface defects on the performance of 2D/3D mixed-dimensional perovskite solar cells (PSCs). To address the limitations of the conventional Interface Defect Density (IDD) model, the Interface Defect Layer (IDL) model has been introduced to more realistically represent the effect of the interface defects and recombination losses. Based on two defect models, a 2D/3D mixed dimensional PSC with a device architecture of $FTO/TiO_2/MAPbI_3/BA_2MA_2Pb_3I_{10}$/Spiro-OMeTAD/Au was simulated. 2D/3D and 3D/ETL interfaces were identified as critical interfaces in device performance degradation in using the IDD model-based simulations. Accordingly, thin IDL (IDL1 and IDl2) were placed at these interfaces, and their thickness and defect density were systematically optimized. A thickness of 1 nm and a defect density of 10^{13} cm^{-3} were identified to be the most effective values for suppressing recombination and improving efficiency. The study reveals that IDL1 (3D/ETL interface) has a significant effect on photovoltaic parameters than IDL2 (2D/3D interface). The IDL model device achieved a simulated PCE of 19.25%, V_{oc} of 0.98V J_{sc} of 24.68 mA/cm^2, and FF of 79.83% at the optimal thickness and defect density values.**

Keywords - 2D/3D mixed dimensional PSCs, interface defects, interface defect layer, stability, SCAPS.

I. INTRODUCTION

Perovskite Solar Cells (PSCs) are leading third-generation photovoltaic technologies, offering higher Power Conversion Efficiency (PCE) along with cost-effective fabrication practices. However, they are suffering from long term operational stability issues upon exposure to high temperatures, humidity and UV radiation [1]. As a solution for that, 2D perovskite materials, proven to be highly stable, are incorporated with 3D perovskite to enhance the stability. The resultant 2D/3D mixed-dimensional perovskite solar cells serve as a promising approach to achieving both high efficiency and improved stability[2-4]. By integrating 2D perovskite layers as a capping layer on 3D perovskites, it facilitates suppressing ion migration, and passivates surface defects enhancing resistance to heat, moisture and UV radiation [4,5].

In conventional 2D/3D mixed dimensional PSCs are formed from several key layers, including the back contact electrode, Hole Transport Layer (HTL), 2D perovskite capping layer, 3D perovskite light harvesting layer, Electron Transport Layer (ETL), Front contact. In this device architecture, there are three pivotal interfaces: 2D/HTL, 2D/3D and 3D/ETL. In the carrier transportation process, photogenerated carriers in the absorber layer are transported through these interfaces to the corresponding electrodes. These interfaces can introduce localized defect concentrations due to structural disorder, lattice mismatch, , and incomplete chemical bonding[6]. They serve as nonradiative recombination centers, disrupting charge flow and drastically reducing the overall device performance [7].

Conventional numerical approaches to solar cell simulation have a tendency to neglect the severe spatial non-uniformity of interfacial defects. Consequently, the impact of localized recombination at interfaces is usually not considered. Addressing this modelling limitation is necessary in order to facilitate accurate device simulation and correct accounting of the effects of the interface defect [8,9].

In this study, a systematic numerical investigation was conducted on a 2D/3D mixed-dimensional PSC employing SCAPS-1D simulation software. First, interface defect density (IDD) sensitivity analysis is performed to identify the most critical interface. Then, an Interface Defect Layer (IDL) approach [9-11] is adopted at the identified interface to match localized recombination zones.

II. METHODOLOGY

A. Device Design

The device is simulated according to the PIN (Positive-Intrinsic-Negative) configuration. Titanium Dioxide (TiO_2) and Spiro-OMeTAD were chosen as ETL and HTL, respectively. These two materials are widely used in SCAPS 1D simulations as they provide well-defined parameters, ensuring the accuracy of solar cell modelling. As 3D perovskite, Methyl Ammonium Lead Iodide ($MAPbI_3$) was selected, and Butyl Ammonium Lead Iodide (n=3) [$BA_2MA_2Pb_3I_{10}$] was inserted as the capping layer. In this device design, Fluorine-doped Tin Dioxide (FTO) and Gold (Au) serve as the front and back electrode contacts, respectively. Fig. 1 illustrates the device architecture of the simulated PSC.

B. Device Simulation

All simulations were carried out using the drift-diffusion model under AM 1.5 Solar Spectrum of SCAPS 1D simulation software. The simulation parameters for the simulation were taken from previously published literature sources as mentioned in Table I. The electron thermal velocity and hole thermal velocity are taken as 10^7 cms^{-1}. The capture cross-section of the hole and electron is $1 \cdot 10^{-15}$ cm^2.

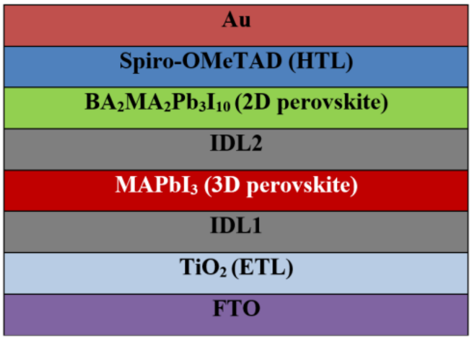

Figure 1. The device architecture of proposed 2D/3D mixed dimensional PSC.

III. RESULTS AND DISCUSSION

A. Effect of Interface Defect Density (IDD) on Different Interfaces (The conventional approach)

In the 2D/3D mixed dimensional PSCs, there are three primary interfaces: 2D/HTL, 2D/3D, and 3D/ETL. The effect of interface defect densities of each interface has been investigated by varying the IDD at each interface. As shown in Fig. 2, a notable difference in the behavior of performance can be observed across the three interfaces. The photovoltaic parameters showed negligible response for the interface defect density variations in the 2D/HTL interface. In contrast, all photovoltaic parameters are highly sensitive to the 3D/ETL interface defect density variation, significantly degrading all the parameters when increasing the defect density. Meanwhile, 2D/3D interface defects show a moderate impact on device performance, resulting in a mild decline in PCE, V_{oc} and FF.

The reasons behind these variations can be explained through interface charge accumulation and recombination. The majority of charge carrier accumulation and recombination happens at the 3D/ETL interface. In addition to that, holes generated within the absorber layers have a higher possibility to successfully reach the HTL without trapping, whereas electrons are more susceptible to being trapped at the 3D/ETL interface [12]. In the 2D/3D interface, there is a balance between charge transportation and the defect-tolerance nature of the 2D perovskite material, which may tolerate severe nonradiative recombination. Hence, the 2D/3D interface exhibits a moderate impact compared to the highly recombination-prone 3D/ETL interface.

TABLE I. INPUT PARAMETERS USED FOR THE SCAPS SIMULATIONS [2,9,13-15].

Parameters	**FTO**	**TiO_2**	**IDL 1**	**$CH_3NH_3PbI_3$**	**IDL2**	**$BA_2MA_2Pb_3I_{10}$**	**Spiro-OMeTAD**
Layer thickness (nm)	500	100	8	Varied	8	1000	30
Bandgap (eV)	3.5	3.26	1.41	1.55	1.41	1.6	2.9
Electron Affinity (eV)	4	4.2	4.17	3.9	4.17	3.87	2.2
Dielectric permittivity (relative)	9	38	8.2	3.2	8.2	5.9	3
Effective density of states of the conduction band C_B (1/cm^3)	$2.2\cdot10^{18}$	$2.2\cdot10^{17}$	$1\cdot10^{18}$	$2.8\cdot10^{20}$	$1\cdot10^{18}$	$7.24\cdot10^{17}$	$2.5\cdot10^{18}$
Effective density of states of the valence band V_B (1/cm^3)	$1.8\cdot10^{19}$	$1.8\cdot10^{18}$	$1\cdot10^{18}$	$3.9\cdot10^{20}$	$1\cdot10^{18}$	$1.5\cdot10^{18}$	$1\cdot10^{19}$
Electron mobility (cm^2/Vs)	20	2·14	1.6	11.8	1.6	1.4	$2\cdot10^{-4}$
Hole mobility (cm^2/Vs)	10	1·13	1.6	11.8	1.6	1.4	$2\cdot10^{-4}$
Shallow uniform donor density N_D (1/cm^3)	$2\cdot10^{19}$	$6\cdot10^{19}$	0	$1\cdot10^{9}$	0	0	0
Shallow uniform acceptor density N_A (1/cm^3)	$1\cdot10^{15}$	0	$1\cdot10^{12}$	$1\cdot10^{9}$	$1\cdot10^{12}$	0	1×10^{18}
Defect density	$1\cdot10^{12}$	$1\cdot10^{12}$	$1\cdot10^{18}$	$1\cdot10^{12}$	$1\cdot10^{18}$	$1\cdot10^{15}$	$1\cdot10^{12}$

Overall, in 2D/3D mixed-dimensional perovskite solar cells, the 3D/ETL interface plays a vital role in charge transport relative to the 2D/HTL interface, making it particularly vulnerable to defect density variations.

B. Effect of Interface Defect Layer (IDL) at the Critical Interface

To make the simulation results more realistic, avoiding the limitations of the conventional interface defect density model, a thin IDL was inserted at the 2D/3D and ETL/3D interfaces, as shown in Fig. 1. The IDL parameters were optimized in terms of both thickness and the defect density. This approach reflects physical degradation at the interface, as supported by previous findings reporting defect-rich zones spreading several nanometers long due to lattice mismatch and chemical instability [11]. Optimization facilitates assessing the device sensitivity to interfacial recombination and enables the identification of tolerable defect levels for efficient performance [8,9].

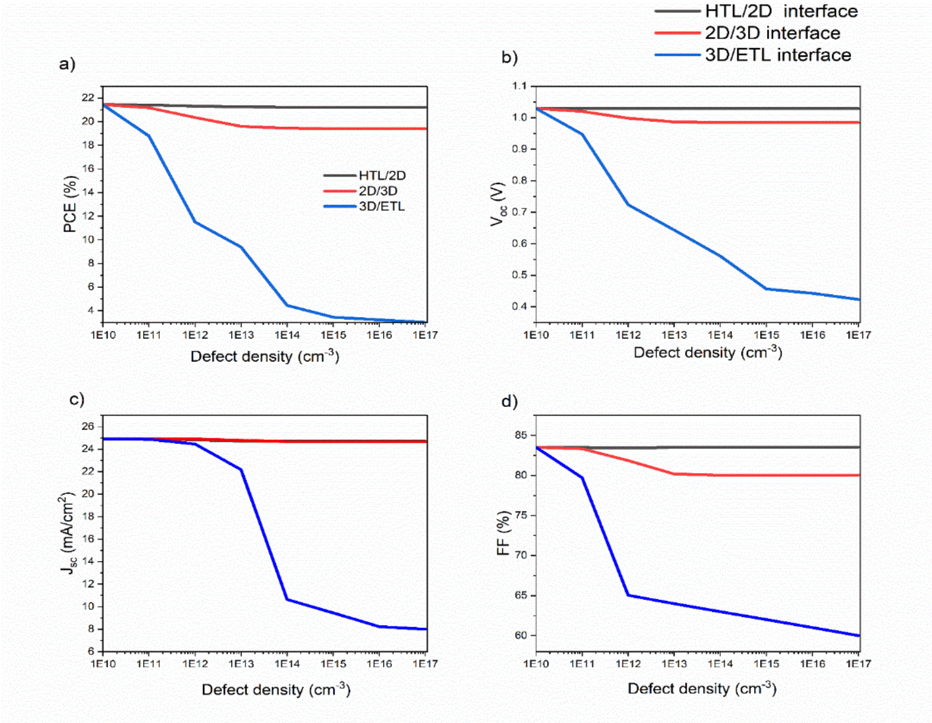

Figure 2. Effect of interface defect density on device performance (IDD model) a) PCE b) Voc c) Jsc and d) FF.

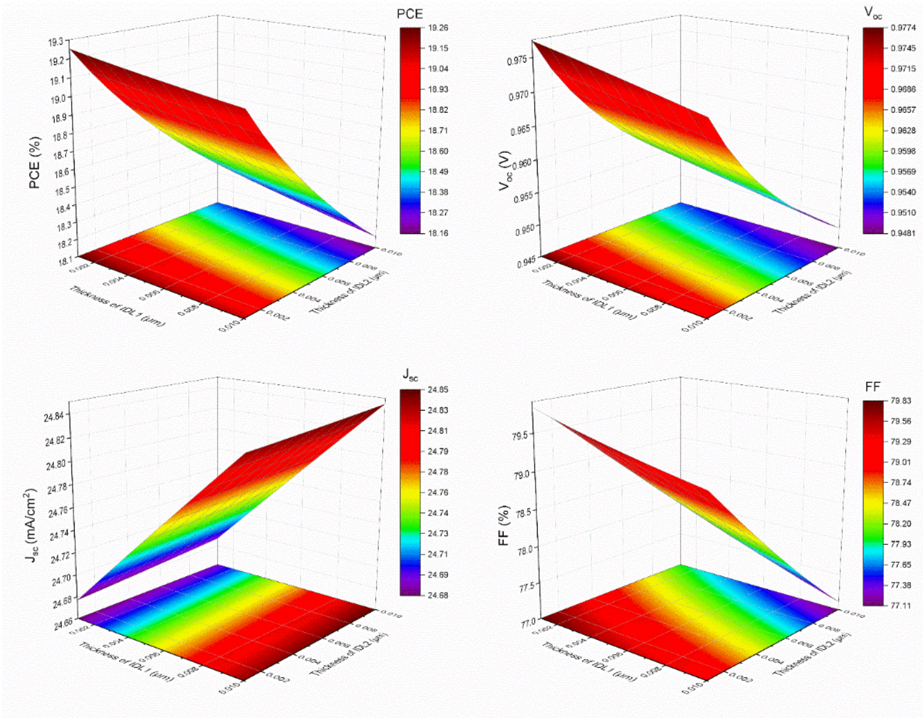

Figure 3. Effect of thickness of IDL on device performance a) PCE b) V_{oc} c) J_{sc} and d) FF.

1) Effect of IDL thickness on the performance of the device

As interface defect acts as charge recombination centers, there is a strong correlation between the performance of PSCs and the interface defect layers IDL1 and IDL2 that are located between the ETL/3D and 2D/3D interfaces, respectively. Based on the given initial parameters, the thickness of IDL1 and IDL2 varied from 1 nm to 10 nm. The resulting performance trends are graphically represented in Fig. 3.

Fig. 3(a) showed the behavior of PCE according to thickness of IDL1 and IDL2. Regardless of the thickness of IDL1, there is no crucial impact on PCE, highlighting the dominant role of IDL2 in determining the performance. As the thickness of IDL2 increases, the PCE has declined from 19.25% to 18.35% at IDL1 thickness of 1 nm. This decline can be attributed to the improved recombination rate of electrons and holes, induced by increased thickness of the interfacial defect layer [9].

When the thickness of the interface defect layer IDL2 is held constant, the V_{oc} shows negligible change when increasing IDL1 thickness, as depicted in Fig. 3(b). However, V_{oc} slightly declines when IDL2 thickness rises, indicating that IDL2 has the principal impact on V_{oc}.

As per Fig 3(c), J_{sc} remains unchanged when increasing the IDL2 thickness. However, J_{sc} slightly increases with IDL1 thickness enhancement. Fig. 3(d) exhibits the response of the fill factor (FF) to the thickness variations. FF declines with the thickness enhancement of both layers. However, compared to IDL1, IDL2 thickness variations have a significant effect on FF. By considering both variations, a 1 nm thickness of both layers has been selected as the optimum thickness value for the next steps of the simulation.

2) Effect of defect densities of the IDL on the performance of the device

Interfacial recombination has a substantial impact on the overall performance of 2D/3D mixed dimensional PSCs. Therefore, to represent realistic device behavior and appropriately address the challenge of quantifying the recombination rates in real devices [9], the impact of defect densities of IDL layers was systematically investigated. The defect densities of both layers varied between 10^{13} - 10^{20} cm^{-3}, keeping the other parameters constant.

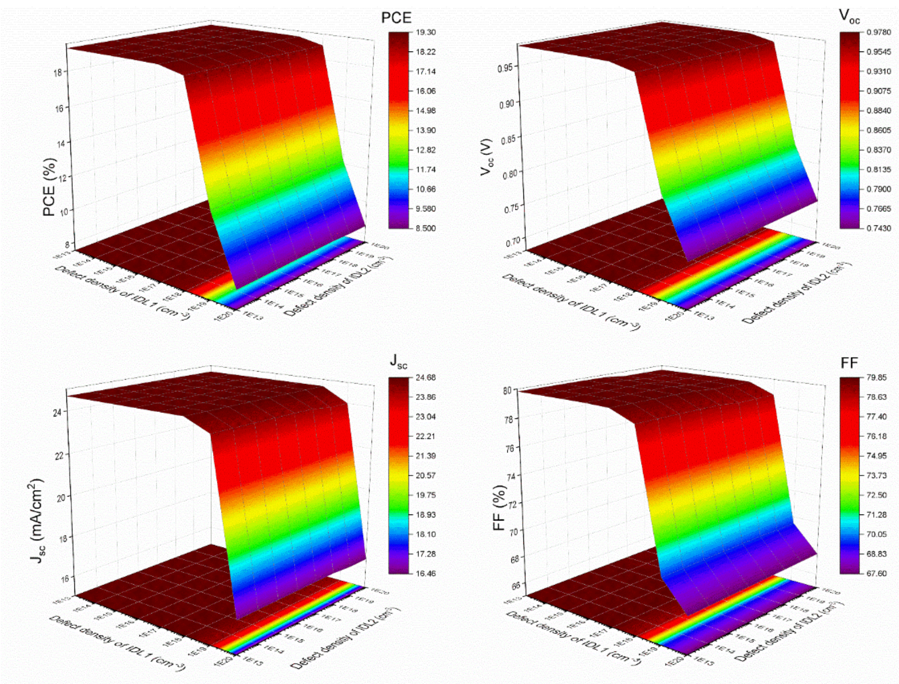

Figure 4. Effect of defect density of IDL on device performance a) PCE b) Voc c) Jsc and d) FF.

The performance trend with varying thickness is plotted in Fig. 4. When the IDL1 defect density increases to 10^{17} cm^{-3}, the device performance remains stable for all IDL1 defect densities. After that, there is a substantial reduction in PCE. However, PCE shows negligible response to the IDL2 defect density variations. Similar behavior can also be seen in the V_{oc}, J_{sc} and FF variations as well highlighting the dominant influence of defect density of IDL1 on performance of the device. Therefore, the optimum defect density for both IDL1 and IDL2 was selected as 10^{13} cm^{-3}.

C. *Comparison Between IDD and IDL Approaches*

By taking the optimum thickness and defect densities of the IDLs, performance of the device is calculated. The IV curves correspond to the two defect models that are illustrated in Fig. 5 and the device performances are mentioned in Table II. The comparative analysis between the interface IDD and IDL approaches reveals considerable differences in photovoltaic performance. In the IDD case, defects are treated as idealized, localized interface traps, which may underestimate the extent of recombination occurring at interfaces of 2D/3D mixed dimensional PSCs.

In the IDL model, a defect region extended for a few nanometers was introduced, which is a better representation of interface degradation, including interdiffusion and structural disorder. This spatially resolved defect region increases the effective recombination volume, resulting in a reduction of V_{oc} from 1.03 V to 0.98 V, and a decline in FF from 83.51% to 79.83%, highlighting greater resistance and recombination losses. The J_{sc} also slightly decreases from 24.92 to 24.68 mA/cm². As a result, PCE drops from 21.43% to 19.25%.

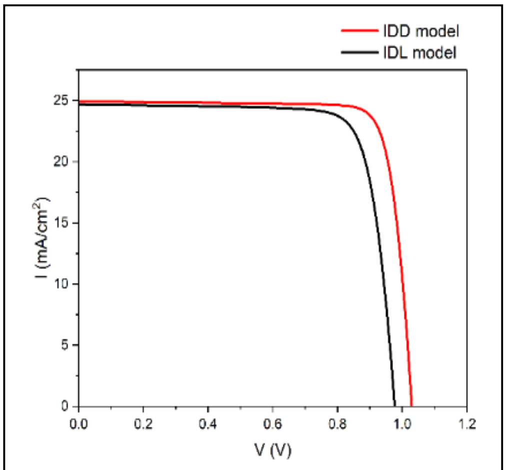

Figure 5. Comparison of the IV characteristics of IDD and IDL models.

In the conventional Interface Defect Density (IDD) model, the interface between two layers-such as the 3D perovskite and ETL-is treated as an infinitesimally thin plane that contains a fixed number of defect states per unit area, denoted by the interface trap density N_{it}.

The carrier recombination at this idealized interface is described by a boundary condition, expressed through the surface recombination velocity S, which quantifies how rapidly carriers recombine at the interface:

$$S = \sigma v_{th} N_{it}, \tag{1}$$

where σ is the carrier capture cross-section (cm²) and v_{th} is the thermal velocity. The recombination current density is expressed as:

$$J_{rec} = qS\frac{(np - n_i^2)}{(n+p)}, \tag{2}$$

where S is surface recombination velocity, n, p electron and hole concentrations, n_i is the intrinsic carrier concentration, and q is the elementary charge.

This relation acts as a boundary condition linking carrier fluxes on either side of the interface:

$$\begin{aligned} J_n\left|x_0^- J_n\right|x_0^+ &= qS(n - n_0) \\ J_p\left|x_0^- J_p\right|x_0^+ &= qS(p - p_0) \end{aligned}. \tag{3}$$

Thus, recombination is confined to a two-dimensional plane, and all defect effects are represented by the single parameter S.

Because the IDD model treats the interface as zero-thickness, it cannot capture spatially distributed defects, interdiffusion, or lattice disorder extending a few nanometers into adjacent layers. As a result, it often underestimates recombination losses and interface degradation effects.The proposed Interface Defect Layer (IDL) model, in contrast, introduces a finite layer of thickness of 1–10 nm with distributed trap states of density. Within this region, recombination follows Shockley-Read-Hall (SRH) statistics, modifying the carrier continuity equations to include volumetric recombination terms. This allows spatially resolved treatment of recombination losses and electrostatic potential variations, providing a physically realistic depiction of interfacial degradation. Within the IDL, recombination is governed by the Shockley-Read-Hall (SRH) mechanism, and the recombination rate per unit volume is expressed as per Eqs. (4) and (5) [2].

$$R_{SRH} = \frac{np - n_i^2}{\tau_p(n+n_i) + \tau_n(p+p_i)}, \quad (4)$$

$$\tau_{n,p} = \frac{1}{\sigma v_{th,n,p} N_t}. \quad (5)$$

Here, R_{SRH} represents the rate of the Shockley–Read–Hall recombination, n and p are the concentrations of electrons and holes, respectively. τ_p, τ_n are the lifetimes of the electron and hole. υ_{th}, n, p are the thermal velocities of electrons and holes, respectively. The carrier continuity equations inside the IDL region are modified to include the volumetric recombination term as shown in Eqs. (6) and (7).

$$\frac{dJ_n}{dx} = q(G - R_{SRH,IDL}), \quad (6)$$

$$\frac{dJ_p}{dx} = -q(G - R_{SRH,IDL}), \quad (7)$$

where G is the generation rate.

At the boundaries of the IDL, both carrier current densities and potentials are continuous as Eqs. (8) and (9):

$$J_n(ETL) = J_n(IDL) = J_n(3D), \quad (8)$$

$$\phi(ETL) = \phi(IDL) = \phi(3D), \quad (9)$$

where ϕ represents the electrostatic potential in the semiconductor.

This formulation treats the interface not as a discontinuity, but as a transition region where defects influence carrier transport and recombination in a spatially resolved manner. The quantitative comparison of these two models (Table II) shows a 2.18 % reduction in PCE, and a 0.05 V drop in V_{oc} in the IDL case, arising from the extended recombination region. Thus, the IDL model more accurately captures non-ideal interface behavior resulting from interdiffusion, lattice mismatch, and defect clustering.

TABLE II. COMPARISON OF THE PERFORMANCE OF DEFECT MODELS.

Device	**PCE (%)**	**V_{oc} (V)**	**J_{sc} (mA/cm^2)**	**FF (%)**
IDD	21.43	1.03	24.92	83.51
IDL	19.25	0.98	24.68	79.83

IV. CONCLUSION

This study offers a comprehensive analysis of the impact of interface defects on the performance of 2D/3D mixed dimensional PSCs. To address the limitations associated with the conventional defect model. The Interface Defect Layer (IDL) model is introduced to represent the recombination process more realistically. The initial IDD model identified the 2D/3D and 3D/ETL interfaces are crucial for the device performance. Therefore, IDL layers were introduced in these two interfaces and the thickness and the defect density of the IDLs were optimized. A thickness of 1 nm and a defect density of 10^{13}cm^{-3} were determined to be optimum values, as they correspond to the highest device performance in terms of PCE, V_{oc}, and J_{sc}. The thickness and defect density of IDL1 have a more pronounced impact on the efficiency of the device compared to IDL2. The marked performance difference between the conventional IDD and the refined IDL models underscores the importance of advanced defect modeling in the design and simulation of 2D/3D mixed-dimensional PSCs.

REFERENCES

[1] Li, X., et al. (2023). Mixed perovskites (2D/3D)-based solar cells: A review on crystallization and surface modification for enhanced efficiency and stability. *Advanced Composites and Hybrid Materials*, 6(3), 1-27.

[2] Chaurasia, S., et al. (2024). Highly efficient and stable Dion–Jacobson (DJ) 2D–3D perovskite solar cells with 26% conversion efficiency: A SCAPS-1D study. *Journal of Physics and Chemistry of Solids*, 191, 112038. https://doi.org/10.1016/j.jpcs.2024.112038

[3] Gamage Ayomi Pabasara, W., & Asha Sewvandi, G. (2025, January 20). Numerical simulation and

optimization of stable CH_3 NH_3 PbI_3 -based 2D/3D mixed dimensional perovskite solar cell. In *Proceedings of10th Virtual International Conference on Science, Technology and Management in Energy (eNergetics 2024), Virtual.*

[4] Lin, T., Dai, T., & Li, X. (2023). 2D/3D perovskite: A step toward commercialization of perovskite solar cells. *Solar RRL*, 7(7), 1-28. https://doi.org/10.1002/solr.202201138

[5] Chen, P., Bai, Y., Wang, S., Lyu, M., Yun, J. H., & Wang, L. (2018). In situ growth of 2D perovskite capping layer for stable and efficient perovskite solar cells. *Advanced Functional Materials*, *28*(17), 1-10.

[6] Abbas, M., Xu, X., Rauf, M., & Kyaw, A. K. K. (2024). A comprehensive review on defects-induced voltage losses and strategies toward highly efficient and stable perovskite solar cells. *Photonics*, *11*(1). https://doi.org/10.3390/photonics11010087

[7] Tao, J., et al. (2024). Suppressing nonradiative recombination for efficient and stable perovskite solar cells. *Energy & Environmental Science*, *17*, 509-544.

[8] Meng, X., et al. (2022). Optimization of germanium-based perovskite solar cells by SCAPS simulation. *Optical Materials*, *128*(May), 112427. https://doi.org/10.1016/j.optmat.2022.112427

[9] Zhang, X., et al. (2023). Germanium–lead double absorber layer perovskite solar cells: Further performance enhancement from the perspective of device simulation. *Optics Communications*, *530*(2103), 129188. https://doi.org/10.2139/ssrn.4171612

[10] Ou, M., et al. (2024). Dion-Jacobson perovskite solar cells: Further optimize the performance by SCAPS-1D simulation techniques. *Materials Today Communications*, *39*(2103), 108955. https://doi.org/10.1016/j.mtcomm.2024.108955

[11] van Gorkom, B. T., van der Pol, T. P. A., Datta, K., Wienk, M. M., & Janssen, R. A. J. (2022). Revealing defective interfaces in perovskite solar cells from highly sensitive sub-bandgap photocurrent spectroscopy using optical cavities. *Nature Communications*, *13*(1). https://doi.org/10.29363/nanoge.hopv.2022.127

[12] Jayawardane, S. T., et al. (2024). Simulation-based performance analysis of lead-free bismuth perovskite solar cells: A comparative study of Cs3Bi2I9 and (CH3NH3)3Bi2I9-based perovskite solar cells. *Advanced Theory and Simulations, 7*(7), 2400206.

[13] Pabasara, W. G. A., Akmal, U. K. D. M., Wickramaarachchi, W. A. A. S., & Swvandi, G. A. (2024). Numerical simulation of lead-free bismuth chalcohalide-based perovskite solar cells. In *Moratuwa Engineering Research Conference (MERCon)*, 436-441. https://doi.org/10.1109/mercon63886.2024.10689236

[14] Mohammed, M. K. A. A., et al. (2023). Harnessing the potential of Dion-Jacobson perovskite solar cells: Insights from SCAPS simulation techniques. *Journal of Alloys and Compounds*, *963*, 171246. https://doi.org/10.1016/j.jallcom.2023.171246

[15] Chakrabartty, J., Islam, M. A., & Reza, S. (2021). Performance analysis of highly efficient 2D/3D bilayer inverted perovskite solar cells. *Solar Energy*, *230*(October), 195-207. https://doi.org/10.1016/j.solener.2021.10.007